Malaysian Journal of Analytical Sciences, Vol 23 No 6 (2019): 938 - 949
DOI: https://doi.org/10.17576/mjas-2019-2306-03

MALAYSIAN JOURNAL OF ANALYTICAL SCIENCES
Published by The Malaysian Analytical Sciences Society
ISSN 1394 - 2506

PREPARATION AND CHARACTERISATION OF HYDROXYAPATITE EXTRACTED FROM FISH SCALE WASTE FOR THE REMOVAL OF GALLIC ACID AS INHIBITOR IN BIOFUEL PRODUCTION

(Penyediaan dan Perincian Hidroksiapatit yang Diekstrak daripada Sisa Sisik Ikan untuk Penyingkiran Asid Galik sebagai Perencat dalam Pemprosesan Bahan Api Bio)

Nurul Fakhriah Ismail[1], Sofiah Hamzah[1]*, Nurul Ashraf Razali[1], Wan Mohd Hafizuddin Wan Yussof[2], Nora'aini Ali[1], Abdul Wahab Mohammad[3]

[1]*Faculty of Ocean Engineering Technology and Informatics, Universiti Malaysia Terengganu, 21300 Kuala Nerus, Terengganu, Malaysia*
[2]*Faculty of Chemical and Natural Resources Engineering, Universiti Malaysia Pahang, Lebuhraya Tun Razak, 26300 Kuantan, Pahang, Malaysia*
[3]*Faculty of Engineering and Built Environment, Universiti Kebangsaan Malaysia, 43600 UKM Bangi, Selangor, Malaysia*

**Corresponding author: sofiah@umt.edu.my*

Received: 13 December 2018; Accepted: 20 October 2019

Abstract

Acid pre-treatment of lignocellulosic waste to produce fermentable sugar for the production of bioethanol and biofuel has created phenolic compounds, aliphatic acid, and furfural. These compounds are recognised as inhibitors in the fermentation process, which could reduce the final product yield. This is a preliminary study that is focused on the potential of hydroxyapatite (HAp) extracted from fish scale for the removal of phenolic compounds (gallic acid was used as a model solution). HAp was extracted *via* a modified enzymatic hydrolysis at various temperatures (500 °C, 600 °C, 700 °C, 800 °C, 900 °C, 1,000 °C) and calcined for 4 hours. The extracted HAp was characterised using Fourier transform infrared spectroscopy (FTIR), X-ray diffraction (XRD), and scanning electron microscope (SEM). Batch adsorption was conducted to select the best adsorbent and to study the effects of initial concentration, time, dosage, and temperature. The results showed gallic acid removal of 78.9% in 100 mg/L of initial gallic acid concentration, which were adhered by HAp800. This adsorption process fit the Freundlich isotherm (r^2 = 0.9951) better than to Langmuir isotherm. The kinetics of adsorption most fitted the pseudo-second order (0.996).

Keywords: batch adsorption, Langmuir, Freundlich, first-order, Pseudo-second order

Abstrak

Pra-rawatan asid terhadap sisa lignoselulosa untuk menghasilkan gula boleh tapai dalam penghasilan bioetanol dan bahan api bio telah menghasilkan sebatian fenolik, asid alifatik, dan furfural. Sebatian ini dikenal pasti sebagai perencat dalam proses penapaian yang akan mengurangkan hasil akhir produk. Kajian awal ini adalah bertujuan untuk mengkaji potensi hidroksiapatit (HAp) yang diekstrak daripada sisik ikan untuk menyingkirkan sebatian fenolik (asid galik digunakan sebagai model larutan). HAp diekstrak melalui proses hidrolisis enzimatik yang diubahsuai pada suhu yang berbeza (500 °C, 600 °C, 700 °C, 800 °C, 900 °C, 1000 °C) dan dikalsin selama 4 jam. HAp yang diekstrak telah dianalisis menggunakan spektroskopi inframerah transformasi Fourier (FTIR), pembiasan sinar-X (XRD), dan mikroskop elektron pengimbas (SEM). Penjerapan kelompok dilakukan untuk memilih penjerap terbaik dan untuk mengkaji kesan kepekatan awal sampel, masa penjerapan, dos penjerap, dan suhu penjerapan. Hasil kajian menunjukkan sebanyak 78.9% asid galik berjaya disingkirkan dalam 100 mg/L kepekatan awal asid galik yang dijerap oleh HAp800. Proses penjerapan ini isoterma dan kinetik HAp800 dan HAp/Chi berpadanan lebih baik

dengan isoterma Freundlich (r^2 = 0.9951) berbanding dengan isoterma Langmuir. Kinetik penjerapan lebih berpadanan dengan pseudo tertib kedua (0.996).

Kata kunci: penjerapan kelompok, Langmuir, Freundlich, kinetik tertib pertama, kinetik pseudo tertib kedua

Introduction

The world's fossil energy reserves will be depleted within a few decades and the environmental issues are causing major concerns and forcing authorities to find alternative sources of energy. Concern over the adverse economic effect of the depleting energy sources, namely, oil, gas, and coal, has driven the production of biofuel and bioethanol from biomass waste as substitutes. The lignocellulosic hydrolysate of biomass waste (plant-based) consists of fermentable sugar. The fermentation process will produce biofuel and bioethanol *via* anaerobic degradation [1]. However, undesirable compounds, such as phenolic compound, aliphatic acid, and furfural will also be produced due to the extreme condition during acid hydrolysis [2]. As an inhibitor, phenolic compounds will remain unconverted during the process, which would lead to a higher reduction of hydrogen yield, as oppose to other inhibitors [3]. Phenolic compounds will inhibit the process and lead to phenolic-protein precipitation [4]. Thus, several methods have been introduced to overcome this situation, including biological, chemical, and physical methods [5]. Biological methods are rather complicated because enzymes and bacterial strains would be involved. These methods are also ineffective because they are expensive and time consuming. Physical and chemical adsorptions that use adsorbents are the simplest method to remove inhibitors. Natural materials can be utilised as adsorbents, such as activated carbon, chitosan, and biosorbents for the adsorption of organic matters, such as gallic acid and salicylic acid [6]. Gallic acid is a form of phenolic compound that can be found in plant hydrolysate. This study will focus on the adsorption of gallic acid using hydroxyapatite (HAp).

Hydroxyapatite ($Ca_5(PO_4)_3OH$) or calcium phosphate apatite is the main component in hard tissues, such as scales, shells, bones, and teeth [7] and it is abundantly present in nature. HAp has many applications in the biomedical fields for the reconstruction of human bones, as bone implants, dental paste, and bone cement [8]. HAp is chemically stable in a physiological environment, has high biocompatibility, and induces specific biological activity [7]. These traits are suitable for the chromatographic separation of polypeptides and proteins [9]. A recent study employed HAp to remove heavy metals in soil and water [8] and it is widely used in dye removal processes [10]. Zou et al. reported the successful removal of heavy metal ions, including Hg^{2+}, Pb^{2+}, and Zn^{2+} using hydroxyapatite with different morphologies [11]. Alumina-hydroxyapatite composites were also employed for phenol removal in which the hydroxyapatite was extracted from phosphate [12].

Indeed, various methods have been developed to extract natural HAp due to the high cost of commercially available HAp. The extraction of HAp from its natural sources must be taken into consideration. Fish processing industries produce approximately 50% of waste [13], which consists of 4% of fish scales. HAp from fish scales can be synthesised via alkaline hydrolysis [13], enzymatic hydrolysis [14], and hydrothermal hydrolysis [15] methods. Good quality HAp was successfully extracted from biomass, such as shells, animal bones, and fish scales [8]. The present work has extended the findings in the previous study by extracting HAp from fish scales *via* enzymatic hydrolysis for phenolic acid removal.

Materials and Methods

Material

Fish scales (500 g) were collected from local markets around Kuala Terengganu. Protease enzyme from Bacillus complex (Protamex®) and commercial hydroxyapatite were purchased from Sigma-Aldrich. Gallic acid monohydrate ($C_7H_6O_5$) (molecular weight = 170 g/mol) was purchased from ACS reagent. All chemicals are of analytical grades.

Hydroxyapatite sample extraction

Fish scales were collected and washed several times using tap water to remove flesh, gills, and other impurities. Then, the fish scales were dried in static air at 80 °C for 24 hours. The dried fish scales were boiled for 3 hours, while being stirred at 450 rpm using an overhead stirrer. The fish scales were filtered and washed using distilled water. Next, the boiled fish scales were dried at 80 °C for 24 hours. Then, the fish scales were ground into powder

using an analytical mill (IKA A11 basic analytical mill) and the resulting powder was treated with 1% of Protamex® solution for 3 hours in an optimum controlled temperature (40 °C) at pH 9. Next, the mixture was washed with distilled water and centrifuged. The white precipitate that formed was dried at 80 °C for 24 hours and left to cool down to room temperature. The resulting HAp was calcined at different temperatures of 500 °C (HAp500), 600 °C (HAp600), 700 °C (HAp700), 800 °C (HAp800), 900 °C (HAp900), and 1,000 °C (HAp1000) for 4 hours.

Characterisation of HAp

The morphology of the synthesised HAp was studied using a scanning electron microscope (SEM) (JEOL JSM 5410 & JSM 5300, Japan). The samples were first prepared by coating them with gold. Then, the FTIR IRTracer-100 from Shimadzu was used to study the surface functionalities of HAp. The spectra were collected at a range of 4,000 to 400 cm^{-1} with a resolution of 4 cm^{-1}. HAp samples were prepared using the potassium bromide (KBr) pellet method. The crystallographic phases were studied using a Rigaku Mini Flex II desktop X-Ray diffractometer employing 18 kW CuKα radiation, with 45 kV of voltage, current of 40 mA, and λ at 1.5406 Å. Data were collected from 2θ = 20°–80°. Then, the collected data were analysed using search-match software and compared with the powder diffraction data (PDF no-796940).

Batch adsorption study

A model of the phenolic compound was prepared by mixing gallic acid monohydrate and deionised water as solvent. Batch adsorption was conducted at the initial concentration of 50–100 mg/L with different HAp dosages from 1 to 25 g/L. These adsorption reactions were conducted at 10 °C to 60 °C. The samples were shaken for 30 to 480 minutes in an incubator shaker that was set at 240 rpm. Then, the HAp was filtered using Whatman™ 1002-125 filter paper with pore size of 8 µm. The final concentration of gallic acid was quantified using blue Prussian method. The experimental work was repeated three times to ensure the reproducibility of the experimental data. The percentage removal (R_t) of gallic acid at any given time was calculated using the following Eq. (1):

$$R_t = \left(\frac{C_0 - C_t}{C_0}\right) \text{x } 100 \quad (1)$$

where C_0 is the initial concentration of gallic acid (mg/L) and C_t is the concentration of gallic acid at the specific time [9].

The adsorption capacity was calculated using the following Eq. (2):

$$Q_e = V\frac{(C_0 - C_t)}{m} \quad (2)$$

where Q_e is the amount of gallic acid adsorbed at equilibrium (mg/g), V is the volume of gallic acid (L), and m is the mass of adsorbents (g).

Analysis of adsorption isotherm

Langmuir and Freundlich isotherm models were used to analyse the adsorption behaviour of the adsorption process. A comparison between these isotherms is important to develop the equation that will accurately represent the results [16]. These models describe the adsorption based on different assumptions. Langmuir isotherm assumes that the adsorption is homogenous and monolayer, with no interaction between the adsorbed molecules [17].The linear Langmuir equation is presented by the following Eq. (3):

$$\frac{C_e}{Q_e} = \frac{1}{q_m K_L} + \frac{1}{q_m} C_e \quad (3)$$

where C_e is the gallic acid concentration at equilibrium (mg/L), Q_e is the amount of gallic acid adsorbed at equilibrium (mg/g) calculated from Eq. (2), K_L is Langmuir isotherm constant (L/mg), and q_m is the maximum amount of gallic acid adsorbed per unit weight of adsorbent (mg/g) [13]. On the other hand, Freundlich isotherm was developed to recover the constraints of Langmuir isotherm. Freundlich model is an empirical model that is valid

for heterogeneity, which takes into account the multisite adsorption that might exist between the adsorbate molecules [18]. The Freundlich equation and its linear term are presented by the following Eqs. (4) and (5), respectively:

$$Q_e = K_F C_e^{1/n} \tag{4}$$

$$\ln Q_e = \ln K_F + \frac{1}{n} C_e \tag{5}$$

where Q_e is the amount of gallic acid adsorbed at equilibrium (mg/g) calculated from Eq. (2), C_e is the gallic acid concentration at equilibrium (mg/L), K_F is Freundlich isotherm constant (L/mg), and n is the empirical parameter related to the intensity of adsorption, which varies with the heterogeneity of the material. When n values are in the range of $0.1 < 1/n < 1$, the adsorption process is favourable [19].

Kinetic analysis of adsorption

Kinetic analysis of adsorption is a theoretical study that describes the adsorption rate constant of adsorbate to adsorbent, as well as explains the possible reaction mechanisms related to the adsorption [20]. Thus, it is a critical analysis for selecting optimum condition parameters, especially in designing and modelling the process [19]. In this batch adsorption, three mostly used kinetic analyses (first-order, pseudo-second order, and intraparticle diffusion) were applied to the experimental data. First-order kinetic model is mainly used for the adsorption of solute from a liquid solution [13]. The equation is shown by Eq. (6):

$$\frac{1}{q_t} = \frac{K_1}{q_1}\frac{1}{t} + \frac{1}{q_1} \tag{6}$$

where q_1 and q_t are the amounts of gallic acid adsorbed on adsorbent at equilibrium (mg/g) and at various times (t), respectively. K_1 is the rate constant (min^{-1}) of the first-order model for the adsorption process. The graph of $1/qt$ against $1/t$ was plotted. The values of K_1 and q_1 were calculated from the slope and y-intercept, respectively. The pseudo-second order model is usually used to describe the sorption capacity of the solid phase [17]. This model assumes that chemisorption is the main process of the adsorption [21]. Another assumption by this kinetics model is that the removal of solute from the solution could be due to physiochemical interaction with surface adsorption, which is the rate limiting step [20]. The pseudo-second order model is expressed by the following Eq. (7) [22]:

$$\frac{t}{q_t} = \frac{1}{K_2 (q_2)^2} + \frac{t}{q_2} \tag{7}$$

where q_2 is the maximum adsorption capacity (mg/g) for the pseudo-second order adsorption, q_t is the amount of phenol (mg/g) at time t (min), and K_2 is the rate constant of the pseudo-second order adsorption (g/(mg.min)). Values of K_2 and q_2 were calculated from the plot of t/qt against t.

Another kinetic model applied in this study was the intraparticle diffusion model. The equation is expressed by the following Eq. (8):

$$q_t = K_3 t^{1/2} + C \tag{8}$$

where q_t is the amount of gallic acid adsorbed (mg/g) at time t (min), C is the intercept, and K_3 is the intraparticle diffusion rate constant (mg/(g.min$^{1/2}$)). Values of K_3 and C were calculated from the plot of q_t against $t^{(1/2)}$ [16]. According to this model, the graph of q_t versus $t^{(1/2)}$ should be linear or multi-linear if the intraparticle diffusion is involved in the overall adsorption mechanism [23].

Results and Discussion

Characterisation study: Fourier transform infrared

The FTIR analysis was conducted to identify the surface functionalities of HAp samples that were calcined at 500 °C to 1,000 °C. The spectra of HAp prepared in-house were compared with commercial HAp, as shown in Figure 1. The peak appearing at 3431 to 3560 cm^{-1} confirmed the presence of hydroxyl group (OH^-), which indicates that water was adsorbed onto the surface of HAp [13]. Peaks detected at 1436 - 1649 cm^{-1} describe the presence of the carbonate group (CO_3^{2-}). The source of carbonate may originate from CO_2 in atmosphere [24] or it may be from the HAp itself. The stretching bands of OH^- and CO_3^{2-} have decreased with increasing calcination temperature. This condition can be explained by loses of water adsorbed and by decarbonation process (releasing of the CO_3^{2-} group) to calcium oxide [13]. The high intensity of the peak at 978 cm^{-1} to 1093 cm^{-1} suggests the presence of phosphate stretching. The spectrum also shows a strong bend at 550 cm^{-1} to 650 cm^{-1} (phosphate bending).

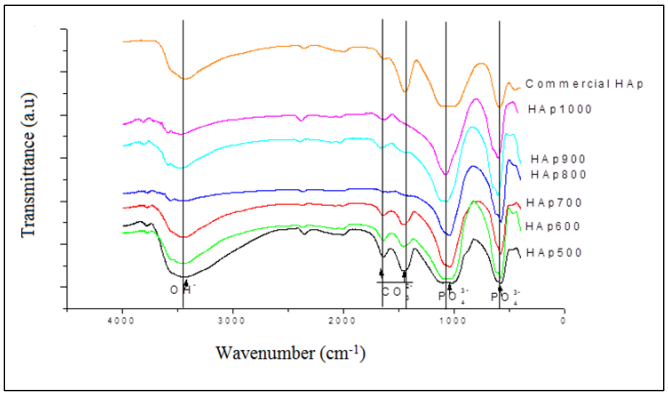

Figure 1. FTIR spectra of commercial HAp and HAp samples prepared in-house, calcined at 500 °C to 1,000 °C

X-ray diffraction

The crystalline phase and intermolecular distances of the HAp was analysed using the wide angle X-ray diffraction (XRD) [22]. The XRD patterns of HAp samples calcined at different temperatures are presented in Figure 2. The XRD patterns show that the peak intensities are improved with increasing calcination temperature. HAp sample calcined at 500 °C shows low crystallinity compared to HAp samples that were calcined at > 800 °C. This change indicates that the HAp sample contains a large amount of organics [25]. The sharp peaks also indicate the crystallinity of the substance, in which the crystallinity of HAp increases with increasing calcination temperature.

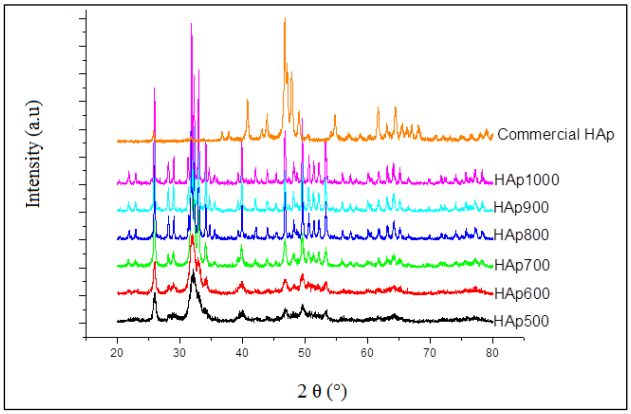

Figure 2. XRD patterns of commercial HAp and HAp samples prepared in-house, calcined from 500 °C to 1,000 °C

Scanning electron microscope

The following Fig. 3 shows the SEM micrographs of HAp samples calcined between 500 °C and 1,000 °C. The morphology of HAp samples extracted from fish scales *via* enzymatic extraction shows irregular shapes and a wide range of particle size distribution.

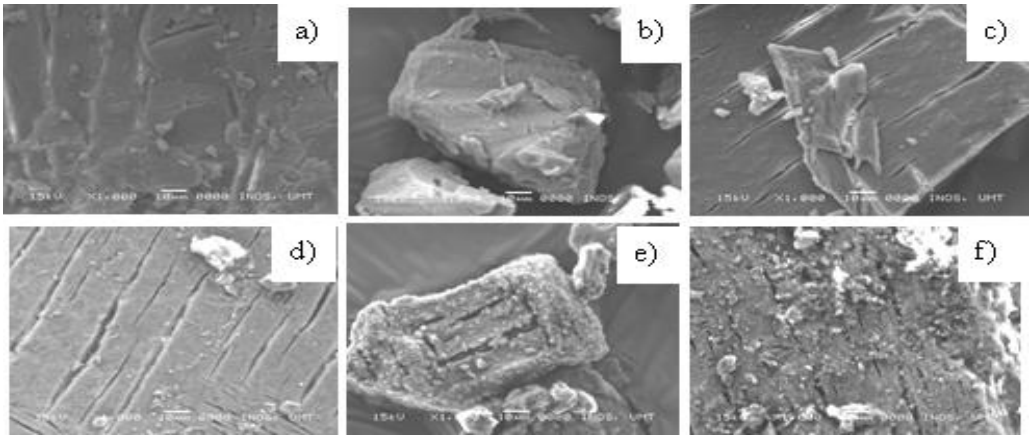

Figure 3. Surface morphology (a) HAp500, (b) HAp600, (c) HAp700, (d) HAp800, (e) HAp900, (f) HAp1000. Magnification is 1000x

Evaluation performance of HAp for gallic acid removal: Effect of calcination temperature of HAp

Different calcination temperatures could influence the properties and performance of the synthesised HAp. Batch adsorption experiments were conducted to determine gallic acid adsorption by each HAp sample, as shown in Figure 4.

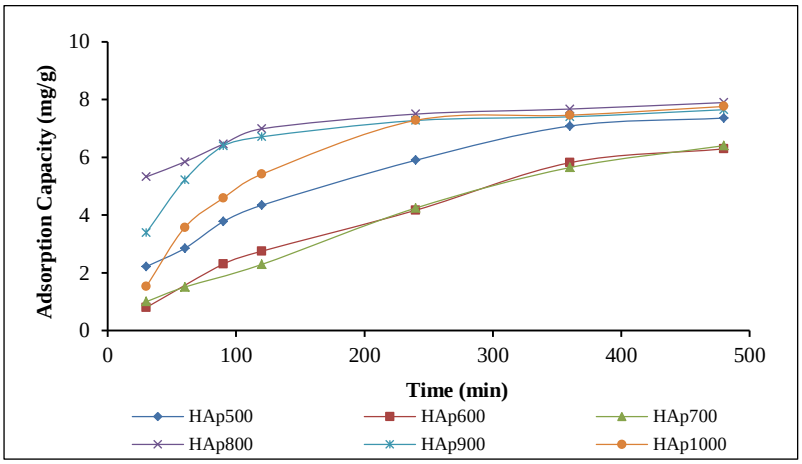

Figure 4. Adsorption capacity of gallic acid by HAp samples produced at different calcination temperatures

Generally, each adsorbent behaved similarly, in which the adsorption process took place in two stages during the kinetic process. The adsorption at the first stage occurred rapidly and became constant in the second stage upon reaching equilibrium. However, HAp samples calcined at higher temperatures (800 °C and above) reached equilibrium at 240 minutes, which was faster than HAp500, HAp600, and HAp700. This experiment showed that HAp800 has the highest adsorption capacity, and thus, was selected for used in the consecutive experiment.

Effect of initial concentration and adsorption isotherm

Langmuir and Freundlich isotherms are commonly used to compare and analyse the behaviour of the isotherm mechanisms. The adsorption process was tested with different initial concentrations of gallic acid solution, from 50 to 100 mg/L using HAp800. The percentage of gallic acid removal had decreased with the increasing initial concentration of gallic acid. In general, the ratio of active sites on HAp for the adsorption to take place and the number of solutes were decreasing with the increasing initial concentration of gallic acid. This situation was due to the higher driving force between the concentration gradient adhered by the high initial concentration and the low initial concentration [25]. The graphs for both Langmuir and Freundlich isotherms were plotted according to Eqs. (3) and (5), respectively, as shown in Figure 5. A summary of isotherm constants is presented in Table 2. Freundlich isotherm fit the experimental data better, with correlation value of $r^2 = 0.995$, in contrast to Langmuir isotherm ($r^2 = 0.876$). The same isotherm was reported in the adsorption of phenolic compounds using activated carbon [26]. This finding also proves that heterogeneous adsorption had occurred, in which the multisite adsorption process was not limited by monolayer formation.

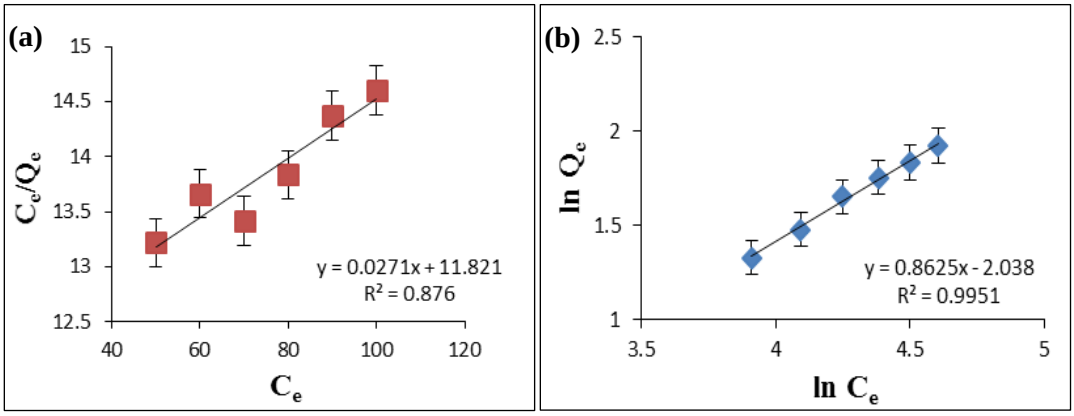

Figure 5. The plotted graphs (a) Langmuir isotherm and (b) Freundlich isotherm for gallic acid adsorption with HAp800 at 60 °C and shaken at 240 rpm

The Freundlich graph shows that the slope value is considerably high (0.862), indicating the high heterogeneity of the adsorbent surface [13]. According to Table 1, the value of n is within $0.1 < 1/n < 1$, which shows that the adsorption is favourable. On the other hand, when the n value is more than 1, this indicates the occurrence of a physical adsorption [16].

Table 1. Langmuir and Freundlich isotherm constants for gallic acid adsorption by HAp800 at 60 °C and shaken at 240 rpm

Langmuir Isotherm		**Freundlich Isotherm**	
r^2	0.876	r^2	0.9951
K_L	2.2925×10^{-3} L/mg	K_F	0.130 (mg/g(L/mg)$^{1/n}$)
q_m	36.90mg/g	$\frac{1}{n}$	0.8625

Effect of time and kinetic analysis

The adsorption was conducted at different time intervals. Gallic acid removal was the highest (78.9%) at 480 minutes upon the introduction of 10 g/L of HAp800 and initial concentration of gallic acid solution of 100 mg/L (Figure 6). The figure shows a sharp increase from minute 30 to 120. The percentage of gallic acid removal showed

a slight increase from 120 to 240 minutes, which became stagnant until 480 minutes. Based on this observation, the equilibrium constant is concluded to be achievable at 240 minutes (74.98%).

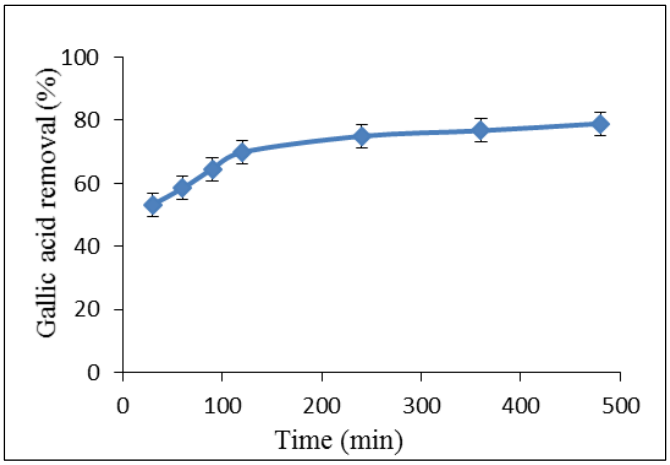

Figure 6. Removal of gallic acid at different reaction times, with initial concentration of 100 mg/L, HAp dosage of 10 g/L, temperature at 60 °C, and shaken at 240 rpm

The experimental data on the effect of time on the percentage of gallic acid removal were used to study the three kinetic adsorption theories: (1) first-order; (2) pseudo-second order kinetic; and (3) intraparticle diffusion. These data are plotted in Figure 7 and the kinetic constant analysis is summarised in Table 2. Both first-order and pseudo-second order models showed good applicability with high values of r^2 of 0.923 and 0.999, respectively. However, the pseudo-second order model fit better with the experimental results since its value of r^2 (0.996) was much closer to unity than the r^2 value of the first-order (r^2 = 0.932) (the results showed the same behaviour, regardless of the adsorption condition). The graph for the intraparticle diffusion model was plotted with two linear lines. According to Cagnon et al., the first linear plot represents the limitation of adsorption by external diffusion, while the last plot represents the final equilibrium [17]. The final equilibrium usually occurs due to the decreased solute concentration in the aqueous solution. According to Figure 7, the adsorption of gallic acid on HAp is predominantly (within 120 min) on the first linear plot. Thus, this adsorption was concluded to be a surface adsorption (external diffusion).

Table 2. Kinetic parameters for the first-order, pseudo-second order, and intraparticle diffusion of gallic acid in the presence of HAp800, with initial concentration of 100 mg/L, temperature at 60 °C and shaken at 240 rpm

	First-order	**Pseudo-Second Order**	**Intraparticle Diffusion**
r^2	0.9236	0.9996	0.8556
k	15.77/min	0.046 g/(mg.min)	0.1316 g/(mg/min$^{1/2}$)
q_e	7.867 mg/g	8.203 mg/g	-
C	-	-	5.0137

Gallic acid adsorption on HAp was assumed to follow the pseudo-second order theory. However, in the capacity of equilibrium adsorption, the first-order model (7.867 mg/g) was closer to the experimental q_e (7.498 mg/g) compared to the pseudo-second order model (8.203 mg/g). The adsorption data were further analysed for the kinetic process using the pseudo-second order kinetic theory.

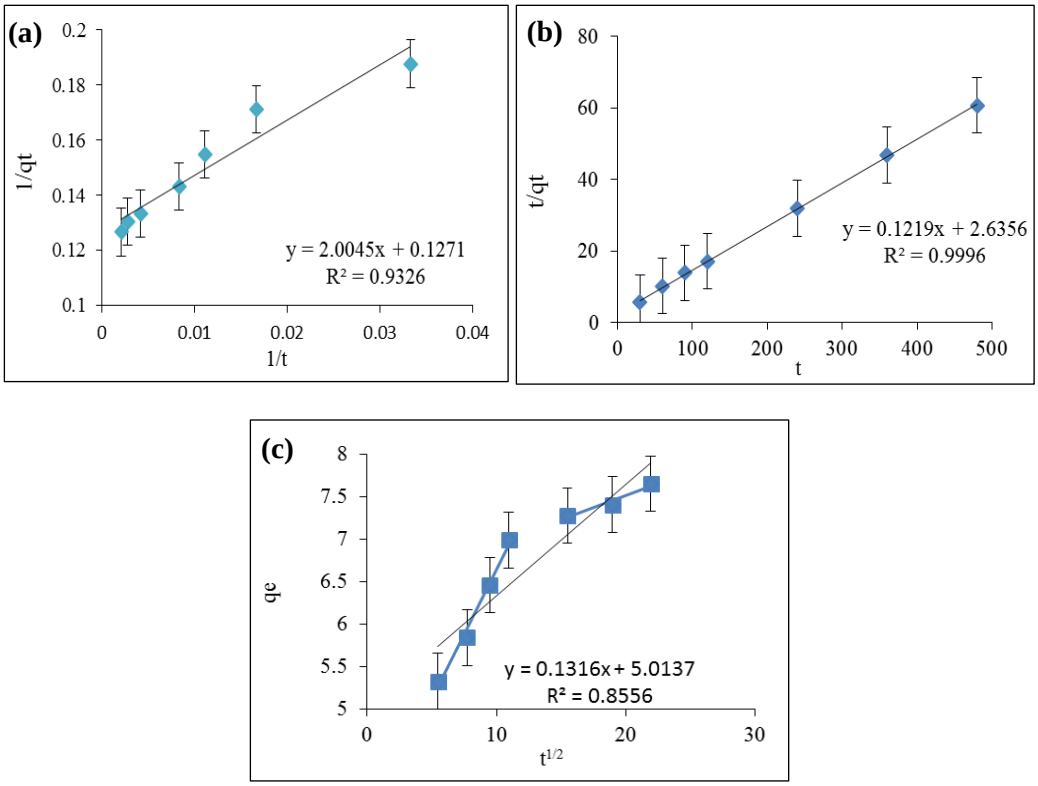

Figure 7. The plotted graphs of (a) first-order kinetic, (b) pseudo-second order kinetic and (c) intraparticle diffusion of gallic acid in the presence of HAp800 and initial concentration of 100 mg/L, temperature at 60 °C and shaken at 240 rpm

Next, the kinetics analysis was conducted by varying the initial concentrations of gallic acid (50–100 mg/L), which were applied on the pseudo-second order model. The adsorption was conducted for 30 to 480 minutes. The maximum adsorption capacity is increased with increasing initial concentration, as shown in Table 3. The experimental work demonstrated that the highest rate constant (0.0109 g/(mg/min)) was achieved from the reaction with initial gallic acid concentration of 50 mg/L. A possible explanation was that the equilibrium adsorption was achieved faster in low initial concentrations. Further analysis showed that during the first 120 minutes, the range of the kinetic constant was double than during the consecutive time. This was due to the abundance of active sites during the earlier time. The number of active sites was decreased over time, leading to a slower adsorption process [26].

Table 3. Pseudo-second order kinetic parameters for different gallic acid concentrations in the presence of HAp800: dosage of 10 g/L, temperature at 60 °C, and shaken at 240 rpm

Initial Concentration (mg/L)	r^2	k **g/(mg/min)**	q_e **(mg/g)**
50	0.9985	0.01090	3.923
60	0.9996	0.00880	4.589
70	0.9981	0.00646	5.593
80	0.9975	0.00573	6.357
90	0.9974	0.00375	7.380
100	0.9977	0.00312	8.347

Effect of dosage

The effect of dosage on the adsorption process was analysed by adding 1, 5, 10, 15, 20, and 25 g/L of HAp to 100 mg/L of gallic acid. According to the graph shown in Figure 8, the percentage of gallic acid removal is increased with increasing HAp dosage, from 1 to 10 g/L. Nonetheless, higher dosage of HAp had shown only a slight increase in the percentage of gallic acid removal. A possible explanation would be that the number of adsorption sites had increased with the increasing HAp dosage. Thus, more active sites were available for the adsorption reaction to take place [17]. In this case, the equilibrium constant was achieved upon the introduction of 10 g/L of HAp dosage, with 79.80% of gallic acid removed. These results were compared to the findings in a previous work. Lin et al. reported that only 28.32% of phenol was removed in the presence of 4 g/L of hydroxyapatite nanopowders, with other similar parameters [12]. On the other hand, the increasing HAp dosage had resulted in the decrease of adsorption capacity. This is because the occupied adsorption site per gram of adsorbent was decreased in high adsorbent dosage. In order to overcome this situation, the initial concentration of gallic acid needs to be increased. In some cases, high dosage is inefficient for the adsorption reaction to take place, which leads to clumps of adsorbents. Thus, it is crucial to study the optimum dosage.

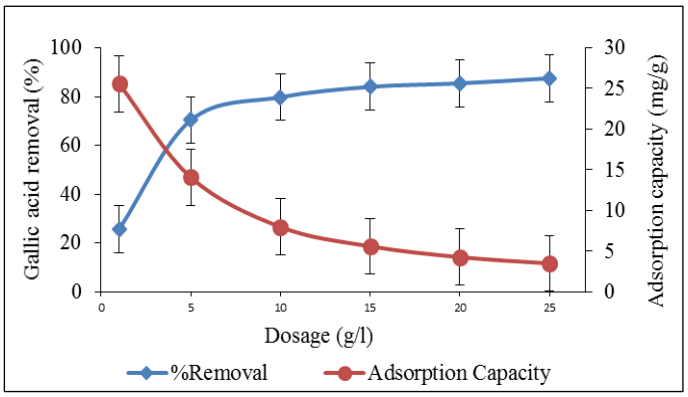

Figure 8. Percentage of removal and adsorption capacity at different HAp dosages. Initial gallic acid concentration = 100 mg/L, temperature = 60 °C, and time = 240 minutes

Effect of temperature

The adsorption reaction was conducted between 10 °C and 60 °C. The adsorption capacity was increased with increasing reaction temperature, as shown in Figure 9. These results indicated that the adsorption reaction had underwent an endothermic process [21]. In addition, these results indicated that the mobility of gallic acid molecules in the solution had increased with increasing temperature.

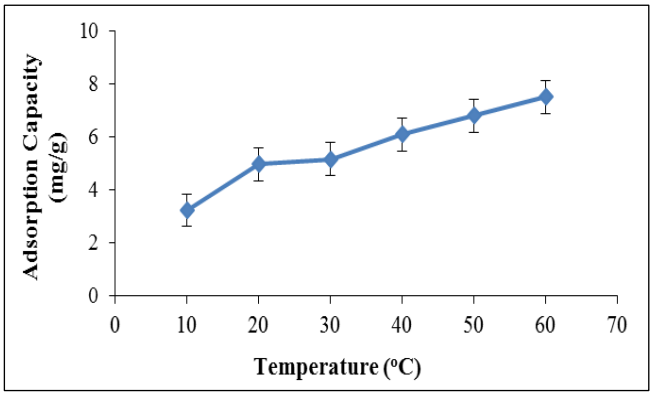

Figure 9. The effect of reaction temperature on the adsorption capacity of HAp800. Initial gallic acid conentration = 100 mg/L, HAp dosage = 10 g/L, time = 240 minutes

Conclusion

HAp was successfully extracted from fish scales using the enzymatic extraction method. HAp samples that were calcined between 500 °C to 1,000 °C employed herein were able to adsorb gallic acid. The percentage of gallic acid removal was the highest (78.9%) at 480 minutes upon the introduction of 10 g/L of HAp800 and the initial concentration of gallic acid solution was 100 mg/L. This adsorption was best fitted with Freundlich isotherm and pseudo-second order kinetics. Thus, this study concludes that this was a heterogeneous process, with multisite adsorption. Meanwhile, the absorption reaction was found to be endothermic.

Acknowledgement

The authors gratefully acknowledge the Ministry of Higher Education Malaysia for the financial support (LRGS Vot no: 53194) and the Central Laboratory of Universiti Malaysia Terengganu for providing equipment and support.

References

1. Prasad, R. K., Chatterjee, S., Mazumder, P. B., Gupta, S. K., Sharma, S., Vairale, M. G. and Gupta, D. K. (2019). Bioethanol production from waste lignocelluloses: A review on microbial degradation potential. *Chemosphere*, 231: 588–606.
2. Lee, J. W., Trinh, L. T. P. and Lee, H. J. (2014). Removal of inhibitors from a hydrolysate of lignocellulosic biomass using electrodialysis. *Separation and Purification Technology*, 122: 242–247.
3. Lin, R., Cheng, J., Ding, L., Song, W., Zhou, J. and Cen, K. (2015). Inhibitory effects of furan derivatives and phenolic compounds on dark hydrogen fermentation. *Bioresource Technology*, 196: 250–255.
4. Kim, Y., Ximenes, E., Mosier, N. S. and Ladisch, M. R. (2011). Enzyme and microbial technology soluble inhibitors/deactivators of cellulase enzymes from lignocellulosic biomass. *Enzyme and Microbial Technology*, 48: 408–415.
5. Palmqvist, E. and Hahn-Hargedal, B. (2000). Fermentation of lignocellulosic hydrolysates I : Inhibition and detoxification. *Bioresource Technology*, 74(1): 17–24.
6. Han, F., Xu, C., Sun, W. Z., Yu, S. T. and Xian, M. (2017). Effective removal of salicylic and gallic acids from single component and impurity-containing systems using an isatin-modified adsorption resin. *RSC Advances*, 7: 23164–23175.
7. Chavan, P. N., Bahir, M. M., Mene, R. U., Mahabole, M. P. and Khairnar, R. S. (2010). Study of nanobiomaterial hydroxyapatite in simulated body fluid: Formation and growth of apatite. *Materials Science and Engineering B: Solid-State Materials for Advanced Technology*, 168(1): 224–230.
8. Piccirillo, C., Pullar, R. C., Tobaldi, D. M., L. Castro, P. M. and E. Pintado, M. M. (2014). Hydroxyapatite and chloroapatite derived from sardine by-products. *Ceramics International*, 40: 13231–13240.
9. Elliott, J. C., Wilson, R. M. and Dowker, S. E. P. (2002). Apatite structures. *Advances in X-Ray Analysis*, 45: 172–181.
10. Nguyen, V. C. and Pho, Q. H. (2014). Preparation of chitosan coated magnetic hydroxyapatite nanoparticles and application for adsorption of reactive blue 19 and Ni^{2+} ions. *The Scientific World Journal*, 2014: 1–9.
11. Zou, X., Zhao, Y. and Zhang, Z. (2019). Preparation of hydroxyapatite nanostructures with different morphologies and adsorption behavior on seven heavy metals ions. *Journal of Contaminant Hydrology*, 226: 103538.
12. Bouiahya, K., Es-saidi, I., El Bekkali, C., Laghzizil, A., Robert, D., Nunzi, J. M. and Saoiabi, A. (2019). Synthesis and properties of alumina-hydroxyapatite composites from natural phosphate for phenol removal from water. *Colloids and Interface Science Communications*, 31: 100188.
13. Kongsri, S., Janpradit, K., Buapa, K., Techawongstien, S. and Chanthai, S. (2013). Nanocrystalline hydroxyapatite from fish scale waste: Preparation, characterization and application for selenium adsorption in aqueous solution. *Chemical Engineering Journal*, 215–216: 522–532.
14. Huang, Y., Hsiao, P. and Chai, H. (2011). Hydroxyapatite extracted from fish scale: Effects on MG63 osteoblast-like cells. *Ceramics International*, 37(6): 1825–1831.
15. Parhi, P., Ramanan, A. and Ray, A. (2006). Hydrothermal synthesis of nanocrystalline powders of alkaline-earth hydroxyapatites, $A_{10}(PO_4)_6OH)_2$ (A=Ca, Sr and Ba). *Journal of Material Sciences*, 41: 1455–1458.

16. Lin, K., Pan, J., Chen, Y., Cheng, R. and Xu, X. (2009). Study the adsorption of phenol from aqueous solution on hydroxyapatite nanopowders. *Journal of Hazardous Materials*, 161(1): 231–240.
17. B Cagnon, B., Chedeville, O., Cherrier, J. F., Caqueret, V. and Porte, C. (2011). Evolution of adsorption kinetics and isotherms of gallic acid on an activated carbon oxidized by ozone: Comparison to the raw material. *Journal of the Taiwan Institute of Chemical Engineers*, 42: 996–1003.
18. Anbia, M., Mohammadi, N. and Mohammadi, K. (2010). Fast and efficient mesoporous adsorbents for the separation of toxic compounds from aqueous media. *Journal of Hazardous Materials*, 176, 965–972.
19. Rengaraj, S., Yeon, J., Kim, Y., Jung, Y., Ha, Y. and Kim, W. (2007). Adsorption characteristics of Cu (II) onto ion exchange resins 252H and 1500H: Kinetics, isotherms and error analysis. *Journal of Hazardous Materials*, 143: 469–477.
20. Robati, D. (2013). Pseudo-second-order kinetic equations for modeling adsorption systems for removal of lead ions using multi-walled carbon nanotube. *Journal of Nanostructure in Chemistry*, 3: 55.
21. Abdelwahab, O. and Amin, N. K. (2013). Adsorption of phenol from aqueous solutions by *Luffa cylindrica* fibers: Kinetics, isotherm and thermodynamic studies. *Egyptian Journal of Aquatic Research*, 39: 215–223.
22. Azmi, N. A. I., Zainudin, N. F., Ali, U. F. M. and Senusi, F. (2015). Adsorption kinetics on basic red 46 removal using *Cerbera odollam* activated carbon. *Journal of Engineering Science and Technology*, 10: 82–91.
23. Smiciklas, I., Dimović, I. and Mitrić, M. (2006). Removal of Co^{2+} from aqueous solutions by hydroxyapatite. *Water Research*, 40(12): 2267–2274.
24. Salimi, M. N., Bridson, R. H., Grover, L. M. and Leeke, G. A. (2012). Effect of processing conditions on the formation of hydroxyapatite nanoparticles. *Powder Technology*, 218: 109–118.
25. Yusof, S. R. M., Zahri, N. A. M., Koay, Y. S., Nourouzi, M. M., Chuah, L. A. and Choong, T. S. Y. (2015). Removal of fluoride using modified kenaf as adsorbent. *Journal of Engineering Science and Technology*, 10: 11–22.
26. Anbia, M. and Ghaffari, A. (2009). Adsorption of phenolic compounds from aqueous solutions using carbon nanoporous adsorbent coated with polymer. *Applied Surface Science*, 255: 9487–9492.